

Chapter 2. Theoretical Background

2.1. Magnetism

The ability of magnetite (Fe_3O_4) to attract iron was recognised around 2500 years ago, making it the earliest magnetic mineral known by humans. The term "magnet" is supposedly derived from the ancient Turkish area of Magnesia, where abundant deposits of magnetite mineral were found. The Greeks also knew that by touching or rubbing a piece of iron with magnetite would turn the iron into a magnet. The development of the electromagnet, which could generate fields far stronger than those generated by natural magnets, is often considered as the foundation for research on magnetic materials.

In this section, giant magnetostrictive materials (e.g., Terfenol-D), which are ferromagnetic at the relevant temperatures, will be the primary subject of discussion here. Atomic magnetic moments are generated by the orbital momentum and electron spins, laying the foundation for the magnetism in magnetic materials. The atomic magnetic moments align below Curie temperature and produce a directional magnetization effect in magnetostrictive materials. Whereas these moments are randomly oriented above the Curie temperature and show zero magnetization as the combined effect of atomic magnetic moments is nullified. The magneto-elastic coupling effect in the magnetostrictive materials laid the basis for magnetostriction. Thus, to describe the behaviour of a giant magnetostrictive material, it is necessary to first examine its magnetic basics. Which includes the brief overview of the concepts of magnetic fields, magnetization, magnetic induction, magnetic energy, magnetization processes, magnetostriction, demagnetization effects, nonlinear hysteresis effects and Maxwell equations. This section will present the basics only relevant to the following study of giant magnetostrictive materials and different unit conventions used in this dissertation.

In addition, several general references [4,56,64] are also provided for the comprehensive discussion of magnetism and magnetostriction.

2.1.1. Magnetic Field

In magnetism, the notion of the magnetic field (H) is considered to be one of the most basic concepts on a macroscopic scale. Almost everyone has experimented with magnets and felt their fascinating attraction and repulsion forces, which arises from the magnet poles. These poles produce a magnetic field around the magnet due to the directionally oriented electron spins and orbital motions inside the material. This magnetic field will exert a force on a neighbouring pole. In a current-carrying conductor, the movement of electric charges is responsible for the generation of a magnetic field and produces a force due to change in the energy in a space volume. The unit of magnetic field in SI and CGS system is defined as A/m and Oersted (Oe), respectively. The conversion between Oersted and A/m is:

$$1 Oe = 79.6 A/m$$

2.1.2. Magnetic moment and Magnetization

The response of magnetic materials to a field is quantified in terms of magnetic moment and magnetization. If a magnet is placed at a random angle in a uniform magnetic field, a torque is exerted on it and tries to get it to align with the field. The moment of this acting torque is called magnetic moment. The magnetic moments in a unit volume (i.e., magnetic moment density) is a constant quantity and used to measure the degree of materials magnetizing capability which is popularly known as magnetization (M) (or intensity of magnetization). Any material composed of atoms possesses a net magnetic moment per atom (i.e., atomic magnetic moments). These atomic magnetic moments, which are parallelly aligned to each other, are distributed over a large volume within the material, known as a magnetic domain. A magnetostrictive material volume is assumed to comprise several domains. When the net

atomic magnetic moment of domains is randomly ordered, the effective magnetization of the material will be zero, and this state of the material is known as demagnetized. Even in a demagnetized condition of material, the atomic magnetic moments in a domain were aligned. In the presence of a field, the net moment of all the magnetic domains tend to align with the field direction, and this process is known as magnetization. The unit of magnetization in SI system is defined as A/m .

2.1.3. Magnetic flux density and hysteresis loops

The presence of a magnetic field (H) in a medium is felt as a force on the moving charge in that medium, widely known as magnetic flux density (B) (or magnetic induction). Magnetic flux density and magnetic field is directly proportional each other and proportionality constant known as permeability. Permeability is a property shared by all medium, which may be constant or variable depending on the medium's magnetizing capacity. For free space medium, the magnetic induction (B) is linear function of the magnetic field (H) and can be written as,

$$B = \mu_0 H \quad (2.1)$$

where, $\mu_0 = 4\pi \times 10^{-7} H/m$ is a universal constant for permeability in free space. The SI unit of magnetic flux density is defined as *webers/m²* or *Tesla (T)*.

However, the magnetic flux density and magnetic field is no longer directly proportional to each other in some mediums such as ferromagnetic and ferrimagnetic materials. This phenomenon can be observed in the typical sigmoid shape experimental BH loops of a ferromagnetic materials, as shown in **Figure 2.1**, and the permeability will not necessarily be a constant value. So, the relation can be written as

$$B = \mu H \quad (2.2)$$

where, μ is permeability of the medium.

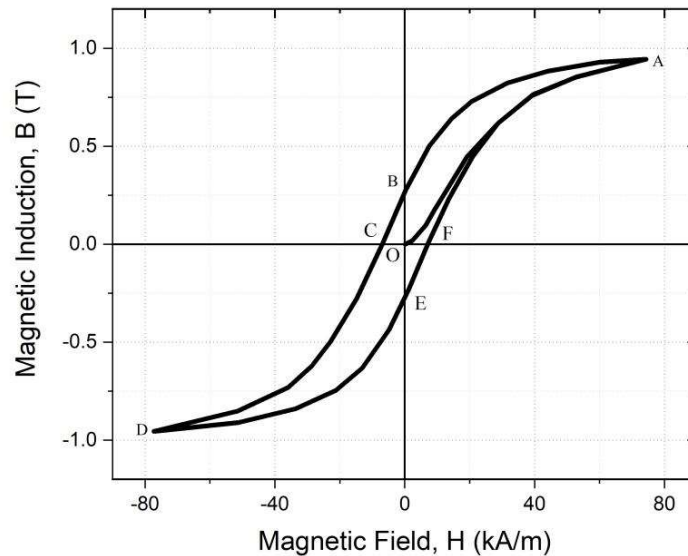


Figure 2.1 Typical experimental B - H loop of a ferromagnetic material

In **Figure 2.1**, when an external magnetic field is initially applied to a demagnetized ferromagnetic material, the magnetic flux density B increases with a steep slope of the initial permeability at point O . At high positive magnetic field (H) values, the material becomes fully magnetized at A , and beyond that the magnetic induction (B) rises with a slope free space permeability. After point A , the magnetic field (H) is reduced to zero and a residual magnetization remains at point B , which is indicated as the magnetic remanence. After point B , the direction of magnetic field is reversed, and the magnetic induction decreased to zero at point C . The additional magnetic field required (i.e., O - C) to attain zero magnetic induction is known as coercivity. On the further decrement in external magnetic field, the material again saturated to negative values of magnetic induction at point D . After point D , on the increment of external magnetic field to the positive saturation values a similar magnetic remanence and coercivity points are encountered at points E and F , respectively. Now, by varying the external magnetic field values in a cycle we can trace the major BH hysteresis loop as A - B - C - D - E - F . The nature of BH hysteresis loop is depends on the

operating conditions. The initial BH loop O-A is not traced in the cycle as the material is not in the demagnetized state to restart the magnetization process. However, it is tedious to model such nonlinear and multi-valued hysteretic curve shape and requires some physics and experiment based explanations.

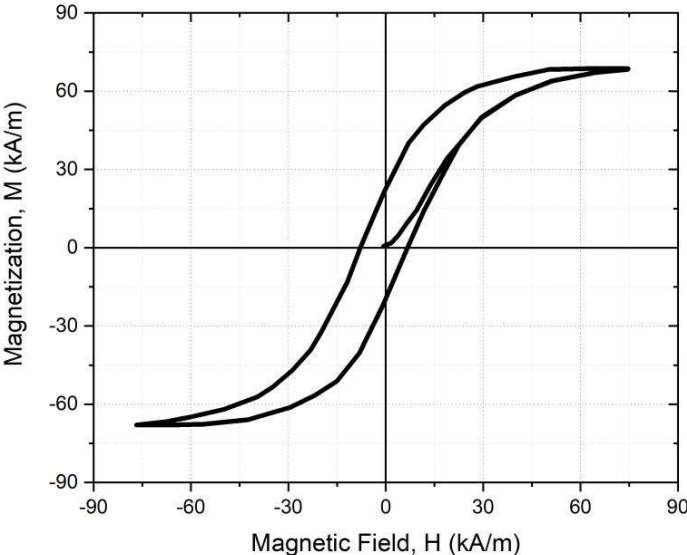


Figure 2.2 A typical M - H curve of a ferromagnetic material

The variations in the permeability can be reasoned to the intrinsic magnetization field M which arises from the parallelly aligned magnetic domains in that medium. The relation between magnetic induction (B), magnetic field (H) and magnetization (M) can be defined as

$$B = \mu_0(H + M) \tag{2.3}$$

The relation between the magnetic field (H) and magnetization (M) is defined as the susceptibility (χ)

$$\chi = \frac{M}{H} = \mu - 1 \tag{2.4}$$

and $\mu = \mu_r \mu_0$, where μ_r is the relative permeability of medium.

Figure 2.2 shows the typical magnetization loop (i.e., M-H curve), will be used as a basis for describing magnetostrictive materials and as an essential component in material constitutive modelling. The slope of MH curve tends to zero at saturation, which denotes a condition where all the magnetic domains are aligned with the direction of the external magnetic field.

2.1.4. Exchange and Magnetic energy

The Weiss' molecular field provides an approximate representation of the exchange interaction energy of quantum mechanics [4]. Weiss (in 1907) postulated that, in magnetostrictive materials, there exists a strong “molecular field”, which is caused by the mutual interatomic interaction. This molecular field, also referred as exchange field, would tend to align the neighbouring atomic magnetic moments parallel to each other. The exchange interaction energies per unit volume at any temperature, can be represented by the contribution of the spatial disuniformities of the magnetization in the free energy, and its tensor form is given as [35,48,65]

$$E^{ex} = \left(\frac{1}{2} \mu_o \eta' \delta_{kl} M_k M_l \right) \quad (2.5)$$

where, δ_{kl} is Kronecker delta, η' is isotropic Weiss molecular field coefficient and i, j, k, l are tensor indices.

Whereas the interaction of domain magnetization with the applied external magnetic field can be defined as the magnetic energy

$$E^m = -\mu_o M_s H_k \quad (2.6)$$

where, M_s is the magnetization within a domain often referred as saturation magnetization.

2.1.5. Demagnetization energy

The demagnetizing magnetic field is generated due to rise in the magnetization within the magnetostrictive material due to shape anisotropy and internal defects, when subjected to applied magnetic field. The magnetostatic energy per unit volume of a dipole of magnetization, when subjected to its own demagnetizing field is referred as demagnetization energy density. This energy reflects the tendency to reduce the total magnetic moment of magnetostrictive material and simultaneously influences the response of magnetostrictive devices. The demagnetization energy density can be expressed as [56,66,67]

$$E^d = \left(-\frac{1}{2} \mu_o N_{kl} M_k M_k \right) \quad (2.7)$$

where, N_{kl} is the demagnetizing factor which is a second rank diagonal tensor. Further, the demagnetization factor ($N = N_{inner} + N_{shape}$) is sum of the inner demagnetizing factor ascribed to the internal defects and the geometric or shape demagnetizing factor due to the shape anisotropy.

2.1.6. Magnetization processes

According to domain theory, the magnetic moments of ferromagnetic materials are aligned even in a demagnetized condition. The difference between magnetize and demagnetize states can be ascribed to a different arrangement of domains in both states. The magnetization process can be reversible or irreversible based on the domain processes involved. A reversible change generally occurs for small field increments, and in such a process, the magnetization attains its original value after removing the applied external field. In most cases, the magnetization does not revert to its original value after the applied field is removed because both reversible and irreversible changes have taken place. Thus, to propose an effective constitutive model of material magnetization, it is necessary to consider the domain processes under the effect of an applied magnetic field.

When an external field is applied to demagnetized state of material, the first type of domain process (i.e., domain rotation) occurs at low fields. In this process, due to the minimization of magnetic energy, certain domains that are aligned with the applied field grow continuously while the size of other domains that are ordered in opposing directions to the magnetic field decreases.

A second type of domain process (i.e., domain wall motion) become relevant at the moderate level of external magnetic fields, in which the net magnetic moment of a randomly oriented domain overcome the magnetic energy and instantly rotate parallel to one of the crystallographic easy directions that is close to the applied external magnetic field direction. The domain wall motion includes two separate effects: domain wall bending and translation. The bending of the domain wall is a reversible process but can become irreversible if the wall meets pinning sites that prevent it from relaxing after the field is withdrawn. Domain wall translation is typically irreversible unless the material is flawless, and the domain wall can reside in a defect-free section of the material.

In the final process (i.e., forced magnetization), on the further increment of the applied field, all the domains aligned with the easy crystallographic direction are gradually rotated in the applied field direction.

Another type of energy that influence the magnetization domain processes, particularly in magnetostrictive materials is the coupled magneto-elastic energy which consider the work done by external stresses. The applied stresses can produce dislocations, which gives rise to regions of inhomogeneous strains within a ferromagnetic solid. These dislocations pin walls of the domain and increases the impedance to domain wall motion.

2.1.7. Magnetic anisotropy

The directional dependence of the measured magnetic properties in a magnetostrictive material is termed as magnetic anisotropy. This factor may strongly influence the shape of BH or MH hysteresis loops. Magnetic anisotropy possesses significant practical interest as it is widely employed in the design of the majority of magnetostrictive materials that are commercially available. Phenomenologically there are three kinds of anisotropy:

1. Crystalline anisotropy
2. Shape anisotropy
3. Stress anisotropy

Out of these anisotropies, only crystalline anisotropy is intrinsically related to the material, while the others are induced. Crystalline anisotropy is arising due to the coupling between electron's spin and orbital motion. When an external magnetic field attempts to realign the electron's spin, the electron's orbit also tends to realign due to spin-orbit coupling. However, the electron's orbit is strongly coupled with the lattice and tries to prevent the rotation of spin axis. Thus, the excess magnetic energy needed to turn the domain's spin system away from the easy direction, is termed as the crystalline anisotropy energy. The spin-orbit coupling is usually considered as weak and requires only few tens of kA/m to overcome it. The magnitude of the anisotropy constants [4,56] (i.e., K_1, K_2 etc.) are used to determine the anisotropy strength in any given crystal and its values decreases rapidly with increment in temperature. Since most materials have a polycrystalline structure and the constituent crystals either randomly oriented or having preferred directional orientation in material. In case of randomly oriented polycrystalline structure, the material will demonstrate no crystalline anisotropy. Whereas, for polycrystalline structure with preferred directional orientation, the material will exhibit crystalline anisotropy. The anisotropy constants for such materials can be determined by the weighted average of every crystal.

If a polycrystalline material having a spherical shape, then it will magnetize to same extent in all directions. But for non-spherical shapes (such as rods, bars, or films), the magnetization of material is not uniform in all directions. In a rod, the application of field along the long axis will magnetized it easily than along the short axis. The disuniformities in the magnetization process arises due to the shape demagnetizing effects as discussed in subsection 2.1.5 and can be a source of a magnetic anisotropy known as shape anisotropy. The magnetization along the short axis, therefore, necessitates a greater magnetic field than that necessary to induce the magnetization along the longitudinal side.

The application of the mechanical stresses can alter the domain orientation of the magnetic material and create a new type of magnetic anisotropy known as stress anisotropy. The application of compressive prestresses on the positive magnetostrictive material lowers the magnetostriction response with respect to applied field. While the tensile stresses increase the magnetostriction response. An entirely opposite phenomenon is observed in the negative magnetostrictive materials. For the detailed explanation on the magnetic anisotropy the reader is referred to the references [4,56,64].

2.1.8. Magnetostriction

The dimensions of a ferromagnetic material change when it is subjected to an external magnetic field. This phenomenon is known as magnetostriction. The magnetostriction of a rod can be express by a special symbol λ to distinguish it from stress induced strain as

$$\lambda = \frac{\Delta l}{l} \quad (2.8)$$

where, Δl is the change in length due to mahnetic filed and l is the original length of material. The value of magnetostriction at magnetic saturation state is denoted as λ_s . This saturation magnetostriction λ_s can be positive or negative and the magnetostriction λ values rely on the applied magnetic field and magnetization effect in material. From the domain theory

perspective, there exists two basic forms of the magnetostrictive strain. First is the spontaneous magnetostriction which results from the alignment of the atomic magnetic moments into domains at the Curie temperature and the other is the magnetic field induced magnetostriction which is usually occurs due to domain rotations. The volume of magnetostrictive materials remains almost same during magnetization of material from demagnetized state to saturation state. Hence, according to the elasticity knowledge the transverse magnetostrictive strain will be almost equal to the one half of the longitudinal magnetostrictive strain as

$$\lambda_t = \frac{-\lambda_s}{2} \tag{2.9}$$

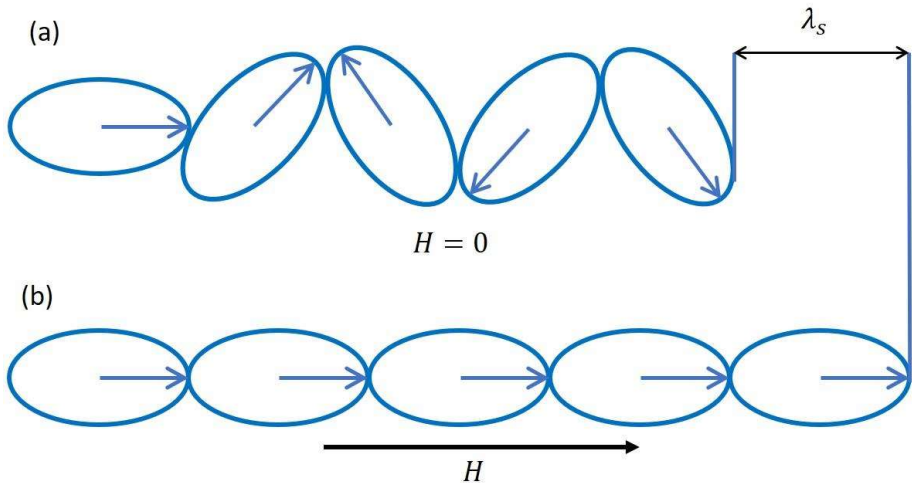


Figure 2.3 Schematic diagram showing the magnetostriction in: (a) the ordered but misaligned demagnetized ferromagnetic regime; and (b) the ordered and aligned ferromagnetic regime, magnetized to saturation.

Thus, magnetostriction mainly originates due to ordering of atomic magnetic moments in the domains, and this process can be depicted in **Figure 2.3**. In this Figure the base of each arrow shows the atomic nucleus, the tip of arrow represents the direction of net atomic magnetic moment, and the oval periphery encloses the non-spherically distributed electrons. The upper row of atoms shows the ordered net magnetic moment but in demagnetize state,

all the atoms are randomly aligned to each other. Upon the application of the external magnetic field, all the atomic magnetic moments become ordered and aligned, and then magnetized to saturation in the lower row.

The stresses also have also an effect on the magnetostriction process. The stresses can rotate the net atomic magnetic moments of the domains inside the magnetostrictive material in a demagnetized state. This property can be exploited to model the magnetostrictive material based devices to enhance the magnetostriction response. Additionally, stresses σ can also alter the easy axis of magnetization, thus it is necessary to consider the stress anisotropy. In addition, magnetostriction causes the Young's modulus E of a magnetostrictive material to vary depending on the strength of the magnetization. This dependency can be explained by the considering a demagnetized material. When a mechanical load is applied to the demagnetized material, two types of strains are produced. First is the elastic strain ε_{el} , that induced in all types of material due to its inherent elasticity. The other type is magneto-elastic strain ε_{me} , which is induced due to the rotation of the magnetic moments of the domains. In the saturated material, the magneto-elastic strain is not produced because there is no scope of further reorientation of domains.

The modulus in the demagnetized condition is due to these two types of strain is

$$E_d = \frac{\sigma}{\varepsilon_{el} + \varepsilon_{me}} \quad (2.10)$$

and the modulus in the saturated condition is

$$E_s = \frac{\sigma}{\varepsilon_{el}} \quad (2.11)$$

These relation gives

$$\frac{\Delta E}{E} = \frac{E_s - E_d}{E_d} = \frac{\varepsilon_{me}}{\varepsilon_{el}} \quad (2.12)$$

The magneto-elastic strain ε_{me} is depends on the applied stress and the crystalline anisotropy. Here the ΔE effect is arising due to an extra contribution of inelastic magneto-elastic strain and the Youngs modulus will be lower than the modulus at saturation.

2.1.9. Maxwell equations

The Maxwell equations with the appropriate boundary conditions are described in this subsection, which are needed to simulate the smart devices based on magnetostrictive materials. The Maxwell equations are composed of four equations, describe the generation and interaction of electric and magnetic fields. These four equations consist of

1. Gauss's law for static electric fields.
2. Gauss's law for static magnetic fields.
3. Faraday's law which states that the variation of magnetic field with time (t) generates an electric field and currents. These electric currents are known as eddy currents.
4. Ampere-Maxwell's law which states that the variation of electric field with time (t) generates a magnetic field.

The magnetic and electric variables used in these equations are magnetic flux density (B), magnetic field (H), electric flux density (D), electric field (E), free electric charge density (ρ_e) and current density (J). The relationships among these variables are summarized by the Maxwell's equations in partial differential form as [68–70]

$$\Delta \cdot \mathbf{D} = \rho_e \quad (2.13)$$

$$\Delta \cdot \mathbf{B} = 0 \quad (2.14)$$

$$\Delta \times \mathbf{E} = -\frac{\partial \mathbf{B}}{\partial t} \quad (2.15)$$

$$\Delta \times \mathbf{H} = \mathbf{J} + \frac{\partial \mathbf{D}}{\partial t} \quad (2.16)$$

The Maxwell equations are used in combination with some constitutive laws for isotropic materials, can be written as

$$\mathbf{J} = \sigma_e \mathbf{E}, \quad \mathbf{B} = \mu \mathbf{H}, \quad \mathbf{D} = \epsilon \mathbf{E} \quad (2.17)$$

where σ_e is the electrical conductivity, μ is the magnetic permeability and ϵ is the dielectric constant of the material. These parameters may be linear or nonlinear quantities depending on the behaviour of material and if the properties are nonlinear, the parameters can become the function of other depending variables. As well, these parameters can be represented in the form of tensors for anisotropic materials.

It is necessary to reduce the complexity of the Maxwell equations to simplify the analysis in particular conditions. The simplifications mainly based on the time dependency of the variables as displayed in equation (2.16) and (2.17). In a static magnetic field condition, the electric field and time dependent quantities in Maxwell's equations vanishes. The Maxwell equations reduced to a pair of equations for magnetostatic fields and illustrates that static magnetic fields can exist in the absence of electric fields. The magnetostatic fields are generated by steady (DC) currents in electromagnets or permanent magnets. The Maxwell's equations for magnetostatic fields can be written as

$$\Delta \cdot \mathbf{B} = 0 \quad (2.18)$$

$$\Delta \times \mathbf{H} = \mathbf{J} \quad (2.19)$$

2.1.10. Magnetic scalar and vector potentials

The Maxwell equations provide the theoretical foundation for the investigation of the relationship between electric and magnetic field variables. Nevertheless, solving Maxwell's equations in the form given in the preceding subsection ((2.13)-(2.16)) is an exceptionally complicated problem. The application of magnetic potentials reduces the complexity and number of equations to solve by transforming some of the variables in such a manner that

some of the equations are identically satisfied [68]. When a vector quantity's divergence becomes zero, the vector quantity can be defined as the curl of the vector potential. In contrast, if the curl of a vector quantity becomes zero, then the vector quantity can be defined as the gradient of the scalar potential. For example, an electric field in electrostatics can be defined as gradient of an electric scalar potential (φ_e) as $E = -\nabla\varphi_e$ when the curl of electric field becomes zero. According to the aforementioned reasonings, two potentials are often employed for the solution of Maxwell equations that are the vector magnetic potential and scalar magnetic potential.

If electric currents are the sole contributor to produce magnetic fields in material, then by using equations (2.18)-(2.19) for divergence free magnetic field, *the vector magnetic potential* (A) can be written as

$$\mathbf{B} = \Delta \times \mathbf{A} \quad (2.20)$$

and by using the equation (2.20) in (2.15), Faradays law can be expressed as

$$\Delta \times \left(\mathbf{E} + \frac{\partial \mathbf{A}}{\partial t} \right) = 0 \quad (2.21)$$

Here, the curl of effective electric field $\left(\mathbf{E} + \frac{\partial \mathbf{A}}{\partial t} \right)$ is vanishes, thus \mathbf{E} can be shown in terms of gradient of the electric scalar potential (φ_e) and magnetic vector potential A as

$$\mathbf{E} = -\nabla\varphi_e - \frac{\partial \mathbf{A}}{\partial t} \quad (2.22)$$

Since, the relationship between \mathbf{J} and \mathbf{E} for a metallic conductor specified by the conductivity σ_E , i.e., $\mathbf{J} = \sigma_E \mathbf{E}$. The introduction of the Faraday law in the Amperes law provides a strong form equation for magnetic field \mathbf{H} and reduces the Maxwell equations for quasi-stationary magnetic field in one equation as

$$\nabla \times \mathbf{H} + \sigma_E \frac{\partial \mathbf{A}}{\partial t} = \mathbf{J}_s \quad (2.23)$$

where $\mathbf{J}_s = -\sigma_E \nabla \varphi$ is source current density and $\sigma_E \frac{\partial \mathbf{A}}{\partial t} = \mathbf{J}_e$ is the eddy-current term. Here, the magnetic field H must be computed as a function of B (or $\Delta \times \mathbf{A}$) using the $B - H$ constitutive relationships. It can be seen from Equation (2.23) that strong form of magnetic vector potential equation is able depict the source currents and eddy currents from dynamic magnetization variations. Thus, the magnetic vector potential extensively used in magnetostrictive devices operated in the quasistatic conditions and exposed to electric currents.

When there is no external or source current density applied, the curl of the magnetic field H vanishes and a magnetic scalar potential φ_m can defined as

$$\mathbf{H} = -\nabla \varphi_m \quad (2.24)$$

The magnetic state of the material can be derived in one equation by substituting Equation (2.24) in (2.14) and using the constitutive relation (2.3) as

$$\nabla \cdot (-\mu_0 \nabla \varphi_m + \mu_0 \mathbf{M}) = 0 \quad (2.25)$$

Thus, the magnetic scalar potential φ_m can utilize the direct constitutive BH or MH relationships in current free magnetic field environments.

2.1.11. Boundary conditions

We can determine the solutions for the differential Maxwell equations given in a domain by using the appropriate boundary conditions associated with that domain. In this subsection, some boundary conditions related to magnetic fields are presented. Consider a source current free interface between two mediums (i.e., medium 1 and 2) having permeability μ_1 and μ_2 respectively, then the boundary conditions can be written as [70,71]

$$\hat{\mathbf{n}} \cdot (\mathbf{B}_1 - \mathbf{B}_2) = 0 \quad (2.26)$$

$$\hat{\mathbf{n}} \times (\mathbf{H}_1 - \mathbf{H}_2) = 0 \quad (2.27)$$

where $\hat{\mathbf{n}}$ is the unit normal vector pointing from medium 2 to 1 as shown in **Figure 2.4**.

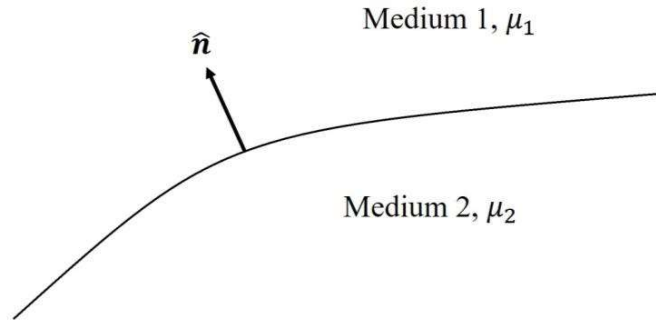


Figure 2.4 Interface between two medium.

Equations (2.26) and (2.27) are derived by assuming that no source current density present at the interface. If required, then Equation (2.27) can be modified as

$$\hat{\mathbf{n}} \times (\mathbf{H}_1 - \mathbf{H}_2) = \mathbf{J}_s \quad (2.28)$$

The modelling domain of magnetostrictive devices in either steady state or transient magnetic fields needed appropriate boundary conditions. Additionally, if the modelling domain possess symmetry, then we can reduce the model size to minimize the computational efforts and time. We can exploit the geometric symmetry and interfacial magnetic boundary conditions to truncate the modelling domain. Two types of interfacial boundary conditions exist as *the magnetic insulation boundary condition* and *the perfect magnetic conductor boundary condition*.

The magnetic insulation boundary condition shows the exactly mirror symmetry plane for magnetic flux density (or magnetic field) and the magnetic field is tangential to the sectioned interface. Thus, the normal component of field can be written as

$$\hat{n} \cdot \mathbf{B} = 0 \quad (2.29)$$

In this boundary condition the tangential part of magnetic vector potential vanishes as

$$\hat{n} \times \mathbf{A} = 0 \quad (2.30)$$

Additionally, this boundary condition imposes antisymmetric condition for electric field and the sectioned interface is perfect electric conductor for surface currents.

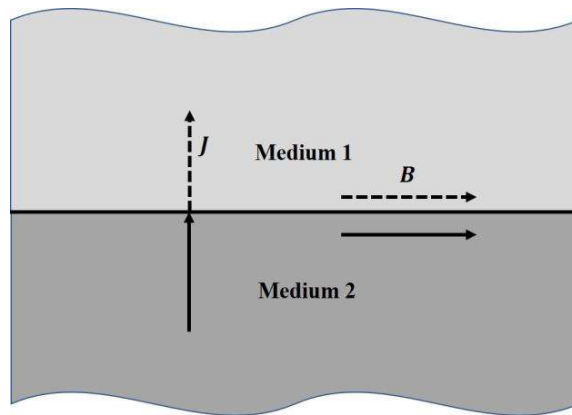


Figure 2.5 The magnetic insulation boundary condition

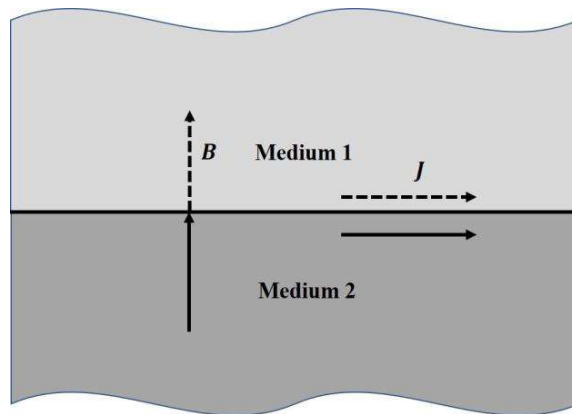


Figure 2.6 The perfect magnetic conductor boundary condition

Whereas *the perfect magnetic conductor boundary condition* presents an exactly mirror symmetrical plane for the electric current and has no normal component. Thus, it can be set

as opposite of the *magnetic insulation boundary condition*. This condition strictly requires the tangential component of the magnetic field to be zero so that the magnetic field only points normal to the sectioned interface and does not change sign as we pass it. This condition can be written in form of magnetic field as

$$\hat{\mathbf{n}} \times \mathbf{H} = \mathbf{0} \quad (2.31)$$

In case of zero current density, this boundary condition can be described in the form of magnetic scalar potential as $\varphi_m = 0$ [24,72–75].

2.2. Nonlinear elasticity

A material is linear elastic if the load required to expand or compress the material by some length is directly proportional to that length. Only two independent constants (e.g., Young's modulus and Poisson ratio) are required to fully define the mechanical response of a linear homogeneous isotropic elastic material. These constants can be derived by using strength experiments and any other material constants can be derived from these two. Many engineering practices benefit from the assumption that materials are linearly elastic under low strains, with possibly nonlinear behaviour due to geometry.

However, many modern active materials deform nonlinearly due to their inherent deformation dynamics and coupled field environment. These active materials are subject of progressive research efforts in sensing and actuation applications and many industrial sectors e.g., automotive, avionics, construction engineering, micro-magneto-mechanical systems, healthcare and automation [1,3,9,10]. For these nonlinear materials, accurate models validated by comprehensive mechanical analysis are required, which may also pave the path for novel applications. In general, only the elasticity constants are not sufficient to describe the mechanical response of nonlinear materials, but it needed some additional nonlinear functions for the deformation. The intricacy of formulating such functions stems from the

fact that stresses (σ) and strains (ε) in nonlinear deformations may be defined in various ways, resulting in several nonlinear functions corresponding to the same linear constant. Moreover, the methodology of an experiment's execution and its data analysis determine which functions are most appropriate [76,77]. For an elastic magnetostrictive material subject to nonlinear strains, the usual approach to optimize the material parameters in the constitutive model is based on basic stress-strain and physics-based experiments [28,52]. Based on their stress-strain curves these materials sometimes can be assumed as linear, bi-linear or non-linear elastic material (or bi-nonlinear) as shown in **Figure 2.7**.

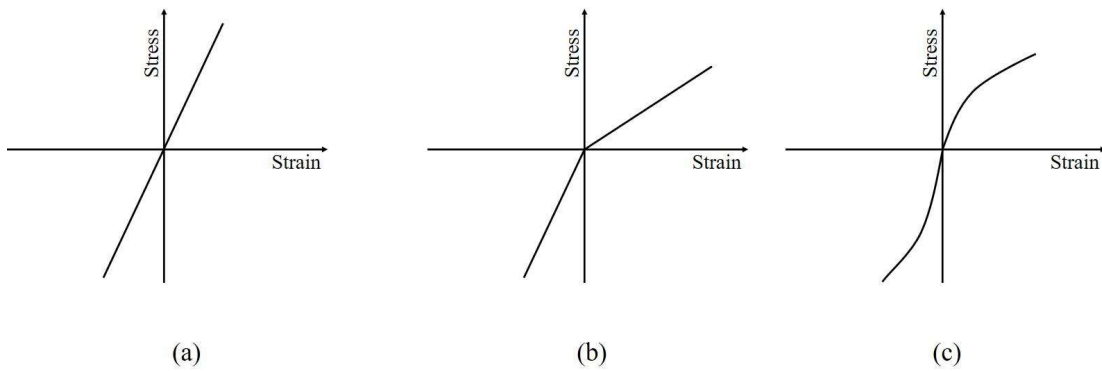


Figure 2.7 Elastic stress-strain curve for (a) linear material (b) bi-linear material and (c) nonlinear material.

2.2.1. Stress-strain relations

The stress-strain relation in a material can be linear, bi-linear, nonlinear, or bi-nonlinear depending on the rate and the nature of coupled field loading. However, most materials employed in the engineering world follow the linear stress-strain relationship given by Hooke's law as

$$\varepsilon_{ij} = S_{ijkl}\sigma_{kl} = \frac{1}{E_{in}} [(1 + \nu)\sigma_{ij} - \nu\sigma_{kk}\delta_{ij}] \quad (2.32)$$

where, S_{ijkl} is conventional compliance tensor, ε_{ij} is the components of strain tensor, σ_{kl} is the components of the stress tensor, and E_{in} and ν are the intrinsic Young's modulus of the

material and the Poisson's ratio, respectively. The relationship between displacements u_i and strain tensor ε_{ij} can be written as

$$\varepsilon_{ij} = \frac{1}{2}(u_{j,i} + u_{i,j}) \quad (2.33)$$

However, nonlinearity can be incorporated in a material by using some additional functions that are based on applied mechanical, thermal, and magnetic loadings as [78]

$$\varepsilon_{ij} = S_{ijkl}\sigma_{kl} + f(\sigma_{ij}, M_l, T) \quad (2.34)$$

Here, $f(\sigma_{ij}, M_l, T)$ is a deformation function of stress, magnetization, and temperature, respectively. A piezomagnetic constitutive model was established [1,5] for the analysis of magnetostrictive materials, which is still most extensively applied in engineering applications. The coupled piezomagnetic constitutive relations can be written as [79]

$$\varepsilon_{ij} = S_{ijkl}^H \sigma_{kl} + d_{kij}^\sigma H_k \quad (2.35)$$

$$B_i = d_{ikl}^\sigma \sigma_{kl} + \mu_{ik} H_k \quad (2.36)$$

where S_{ijkl}^H is conventional compliance tensor at constant magnetic field, d_{kij}^σ is the coupled magneto-elastic constant and μ_{ik} is the magnetic permeability at constant stress. However, the piezomagnetic model is only relevant for a particular bias condition of magnetic field and applied stresses near its operating regime.

2.2.2. Equilibrium equation

All the constitutive relations are limited to define the stress-strain state of the material at one point in the domain but to determine the state of the stress-strain at every point in the domain, one needed equilibrium equations set. Stresses will arise within an elastic body because of the applied loads (which may be dynamic). These internal stresses and the net force acting

on the body must be in dynamic equilibrium. This results in the linear momentum balance equation for the elastic field can be written as

$$\sigma_{ji,j} + f_{bi} = \rho \frac{\partial^2 u_i}{\partial t^2} \quad (2.37)$$

where u_i is displacement, σ_{ji} is stress, ρ is density and f_{bi} is body force per unit volume.

2.3. Magneto-elastic failure

The last several decades have seen a proliferation of novel forms of functional ferromagnetic material, such as magnetostrictive composites and the enormous magnetostrictive alloy of rare earth RE elements. Superior features have led to the use of novel ferromagnetic in the fabrication of sensors, actuators, and transducers. As magnetostrictive materials continue to find applications throughout the engineering spectrum, understanding their mechanical responses to an applied magnetic field is more crucial than ever. Intelligent devices based on giant magnetostrictive materials are now extensively employed in areas such as automotive, avionics, and construction engineering. The dynamic forces by these industrial applications may result in undesirable operating conditions and structural vibrations in intelligent devices. Correspondingly, the area of magneto-mechanics has grown significantly as a discipline. The classical mechanics of ferromagnetic structures has been the subject of extensive study. Traditional studies of magnetoelasticity have focused mostly on the phenomenon of magnetoelastic buckling of ferromagnetic plates. The mechanical behaviour of ferromagnetic plates was carefully investigated by Moon et al [80]. Magnetoelastic buckling of a ferromagnetic plate subjected to a transverse magnetic field was demonstrated for the first time by their tests. To explain the behaviour of a multidomain soft ferromagnetic continuum when exposed to a quasistatic magnetic field, Pao and colleagues [72] used the perturbation technique to develop a linearized magnetoelastic theory based on general nonlinear theory. By solving a system of generic coupled field equations, boundary

conditions, and nonlinear constitutive equations, the linearized magnetoelastic theory was derived. Recent research has focused not only on the buckling of soft ferromagnetic plates, but also on the deformation and fracture of magnetostrictive materials. As giant magnetostrictive alloys of rare earth materials have been developed, some studies [24,26,27] have been conducted to determine the magnetoelastic fatigue-fracture parameters of magnetostrictive materials. This section presents a concise review of the basic theory related to fracture and fatigue mechanics. For detailed discussion regarding fatigue and fracture mechanics, readers can refer [81–84].

2.3.1. Fracture

In order to forecast and diagnose the eventual failure of a magnetostrictive material that already has a crack or imperfection, theory of fracture mechanics is used. Terfenol-D's most significant limitation is its very brittle nature, and in the presence of manufacturing defects, it has a much lower tensile strength than compressive strength [20]. Manufacturing faults such as cracks, cavities, inclusions, de-bonding, and dislocations may concentrate stress near flaws, which might cause the material to fail sooner than anticipated using conventional strength-of-materials techniques.

The early work of Griffith (1921), Orowan (1948), and Irwin (1951) [85–89] established fracture mechanics as an engineering field. Griffith proposed an energy balance approach for the fracture of brittle materials with the introduction of the surface energy term [85], which quantitatively relates the flaw size to the fracture stress by realizing that the relatively low strength and size dependence of strength were due to the presence of crack-like flaws in the materials.

Irwin [86,88] and Williams [90] presents the concept of *stress intensity factor*, which is determined in the field of fracture mechanics by analyzing the relationship between the stress

applied, the flaw size, and the geometry of the component. For a material to fail, the stress intensity factor must be greater than the material's fracture toughness. At this point the crack/flaw will widen rapidly and unpredictably, eventually breaking the component into two. The elasticity of materials consists of three fundamental modes related to crack tip, as seen in **Figure 2.8**. The opening (tensile) mode occurs when the displacements are normal to the crack surface plane, the sliding (in-plane shear) mode occurs when the displacements are parallel to the crack surface plane and normal to the crack front, and the tearing (out-of-plane shear) mode occurs when the displacements are parallel to the crack surface plane and perpendicular to the crack front.

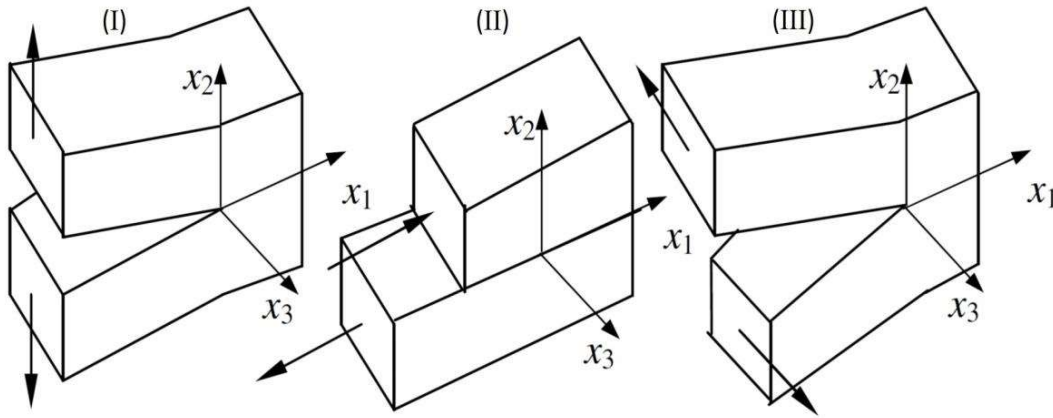


Figure 2.8 Fracture mode (I) Opening mode (II) Sliding mode (III) Tearing mode

For linear elastic brittle material, the stress intensity factor in mode I is defined as

$$K_I = Y\sigma\sqrt{\pi a} \quad (2.38)$$

where Y is a geometrical factor, σ is the applied stress and a is the size of crack. The unit of stress intensity factor is $MPa\sqrt{m}$ and the subscript I is for mode I fracture condition.

Although Griffith [85] was the first to introduce the energy-based approach for the fracture of linear brittle materials, but the modern definition of the energy release rate (sometimes called the strain energy release rate), G , is primarily due to Irwin [86,88].

$$G = -\frac{d\Pi}{dA} = -\left(\frac{\partial U}{\partial A}\right)_\Delta \quad (2.39)$$

where Π is the potential energy of the domain, U is the elastic strain energy, and Δ is the load-point displacement. The initiation of crack growth occurs when G reaches to the critical value G_c .

Based on the ground-breaking work of Eshelby, Cherepanov, and Rice [91–93], the path-independent integrals have been extensively used to investigate the fracture properties of materials having flaws. In a nonlinear elastic body with a flaw, the rate at which energy is released can be represented as a contour integral called the J-integral [94].

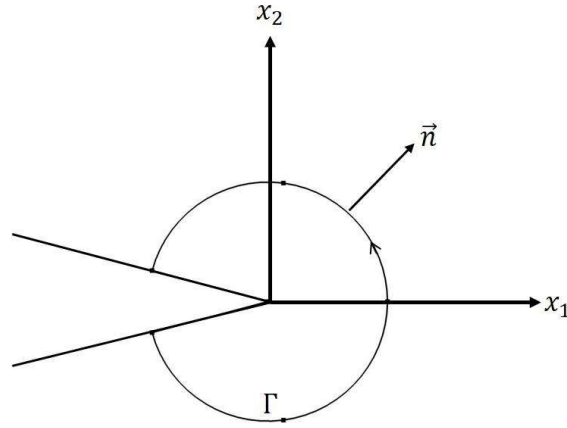


Figure 2.9 Counter-clockwise contour for 2D J-integral

For a counter-clockwise path (Γ) enclosing the crack front in a nonlinear elastic body as shown in **Figure 2.9**, the J-integral is defined as

$$J = \int_{\Gamma} \left(w dx_2 - \sigma_{ij} n_j \frac{\partial u_i}{\partial x_1} ds \right) \quad (2.40)$$

where $w = \int_0^{\epsilon_{ij}} \sigma_{ij} d\epsilon_{ij}$ is the strain energy density, n_j are the components of the unit normal vector, u_i is the displacement vector components and ds is the incremental length along the

contour. The 2D J-integral values for a body is independent of the path around the crack front and the criterion for crack propagation can represent as

$$J = J_c \tag{2.41}$$

where J_c is the critical strain energy release rate.

2.3.2. Fatigue

One of the key problems in many sectors that restricts the widespread implementation of magnetostrictive devices is the long-term service life of giant magnetostrictive material (e.g., Terfenol-D), particularly when subjected to external magnetic field with cyclic loading environment as shown in **Figure 2.10**. When a component disintegrates or collapses after being exposed to several cycles of alternating stress, it is said to have failed through fatigue. Because of high brittleness, low tensile strength, manufacturing flaws, and undesirable operating circumstances; the Terfenol-D based smart sensing devices are susceptible to in-service fatigue-fracture failure in the presence of a magnetic field. As a result, it is critical to analyze the performance of GMMs under such circumstances and to provide a method for estimating magnetostrictive device service life.

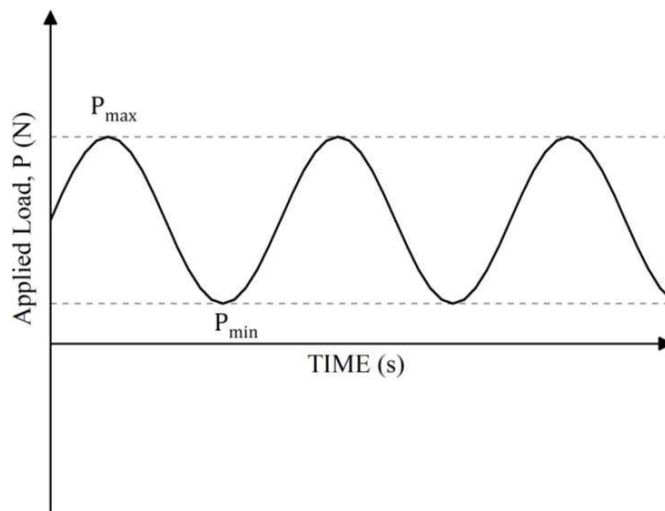


Figure 2.10: Cyclic loading

Although fatigue failures seem to be instantaneous, the process of fatigue-fracture is gradual, starting with crack initiation that expand throughout the life of the material. Under the impact of repetitive low-level load applications, exceedingly small changes occur in the crystalline structure of metals and alloys. The stress concentrations arise due to these small changes produces embryonic crack [95–97]. In fatigue-fracture failure [81], this process is often referred as crack initiation. The crack initiation is followed by the creation of a microcrack, which often occurs along the active slip planes (intergranular fractures are exceptions). Under cyclic stresses, these cracks continue to expand through two separate phases, Stage I and Stage II, eventually leading to catastrophic collapse. There may be several microcracks in a material body at once, and although some of them may never spread at all, others may go through Stage I before arresting or aggregating into remaining cracks, and in most cases only a single microcrack will lead to failure. Stage I crack growth of microcracks is crystallographic in character and propagates along with their slip planes. Stage II crack growth is generally non-crystallographic and originates perpendicular to the applied tensile stress direction. Slip is a shear process, hence slip planes near the maximum shear plane in a component generally favor Stage I growth. Thus, the shear component of applied stress is assumed to drive Stage I crack propagation, whereas the tensile stress part controls the Stage II crack growth. However, once the size of crack is sufficiently enough and the incremental extensions are on the order of defect or particle spacing in a material, the secondary cracking, void formation, and other static fracture modes progressively contribute to crack development. This crack propagation process is caused by a combination of Stage II controlled processes and the static fracture modes and is often referred to as Stage III of fatigue crack propagation. These big flaws continue to expand until the stress in the remaining material section becomes unsustainable, and at that point fracture occurs.

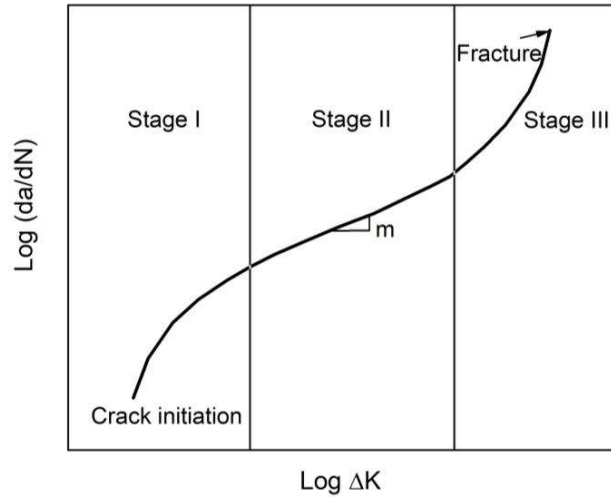


Figure 2.11 Stages of fatigue crack growth

Fatigue-fracture mechanics presents both a graphic and quantitative description of all the three stages of crack propagation, which is known as the Paris and Erdogan [98] curve displayed in **Figure 2.11**. Paris and Erdogan [98] presents the differential approach to quantify the fatigue life. The rate of fatigue crack growth (da/dN) is demonstrated as a function of crack extension force. Here N is the number of cycles spent. Paris and Erdogan use the stress intensity factor range ΔK as crack extension force to propose the relation as

$$\frac{da}{dN} = C \Delta K^m \quad (2.42)$$

This relation is only valid for the middle stage of crack growth curve. Here C and m are the Paris law constants. The constants C and m can assume number of values according to situation. In above equation, ΔK can be written as

$$\Delta K = Y \Delta \sigma \sqrt{\pi a} \quad (2.43)$$

Here, $\Delta \sigma$ can be obtained for maximum and minimum cyclic load (i.e., P_{max} and P_{min} , respectively). A log-log scale is used to plot the Paris curve, with the crack development rate

per cycle (da/dN) on the ordinate (y axis) and the cyclic stress intensity amplitude on the abscissa (x axis), respectively.

However, Chow et al. [99] show that the ΔK alone is not able to adequately characterise the fatigue crack growth behaviour in non-linear elastic materials. The strain energy release rate defined by J-integral (i.e., ΔJ) [99–101] can be used as a physically more reasonable quantity other than ΔK which is recognised as the crack driving force in nonlinear elastic material. Thus the ΔJ can be considered as the primary source for the essential energy dissipated during fatigue crack growth. The Paris and Erdogan relation can be modified as

$$\frac{da}{dN} = C' \Delta J^{m'} \quad (2.44)$$

Here C' and m' are the equivalent Paris law constants. The constants C' and m' can assume number of values according to situation. In above equation, ΔJ can be written as

$$\Delta J = J_{max} - J_{min} \quad (2.45)$$

where, J_{max} and J_{min} can be computed for maximum and minimum cyclic load (i.e., P_{max} and P_{min} , respectively) with the help of Eq. (2.40). Again, a log-log scale can be used to plot the updated Paris curve, with the crack development rate per cycle (da/dN) on the ordinate (y axis) and the cyclic ΔJ amplitude on the abscissa (x axis), respectively.

2.4. Weibull strength theory

Due to the high level of brittleness and low tensile strength of Terfenol-D based smart sensing devices prone to in-service fatigue-fracture failure, particularly in the presence of a magnetic field. The failure and fracture pattern which might be considered stochastic in nature to predict with certainty can therefore compromise its performance. These requirements led to use of probabilistic design methodology, which consists of following major steps:

- 1) Nonlinear elastic fracture mechanics which relates the strength of magnetostrictive materials to orientation, size, and shape of crack, loading conditions and geometry of component.
- 2) An appropriate statistical theory to to characterize the fracture strength of Terfenol-D that fails in a brittle manner.

The Weibull statistical strength theory based on weakest link philosophy was employed to predict the probability of failure (or, alternately, the fracture strength) of the Terfenol-D in magneto-elastic stimuli environment. In the Weibull strength analysis, the three-parameter cumulative probability function for the probability of failure P_f is written as [102,103]:

$$P_f = 1 - \exp \left[- \left(\frac{P_{max} - P_u}{P_\theta} \right)^m \right] \quad P_{max} > 0 \quad (2.46)$$

$$P_f = 0 \quad P_{max} \leq 0 \quad (2.47)$$

where, P_u is the threshold load parameter representing the lowest load value below which test specimen will not fracture. The scale parameter P_θ is the characteristic strength with dependence on the loading configuration. Weibull modulus m is the distribution shape parameter. The three-parameter Weibull model is used to define extreme functions.